

Article

Effect of Black Paste on the Property of Fluorine Resin/Aluminum Infrared Coating

Xiaoxing Yan

College of Furnishings and Industrial Design, Nanjing Forestry University, Nanjing 210037, China; yanxiaoxing@nuaa.edu.cn

Received: 30 August 2019; Accepted: 18 September 2019; Published: 20 September 2019



Abstract: A fluorine resin/aluminum infrared coating was prepared with aluminum using black paste as filler and fluorine resin as binder. The effect of the black paste content on the performance of gloss, color difference, infrared emissivity, hardness, adhesion, impact resistance, roughness, optical testing, and corrosion resistance of the fluorine resin/aluminum infrared coating were examined. When the content of black paste was increased from 1.0% to 9.0%, the gloss of the coating surface decreased; the ΔE^* value of the coating decreased; the infrared emissivity of the coating surface increased gradually; the hardness of the coating was 6H; the adhesion grade of the coating was 0; the infrared absorption peak increased gradually. When the content of black paste was 0%–3.0%, the impact resistance was more than 50 kg·cm, and the impact resistance was higher. When the content of black paste was 0%–5.0%, the surface roughness of the coating was relatively low. When the content of black paste was 1.0%, the corrosion resistance of the coating was the best. The results showed that when the content of black paste was 1.0%, the performance of the whole fluorine resin coating was the best. Through the preparation and characterization of fluorine resin infrared low-emissivity coatings, the possibility of applying fluorine resin to infrared low-emissivity anticorrosive coatings was discussed, which laid a foundation for the subsequent engineering application of coatings.

Keywords: black paste; aluminum powder; fluorine resin; coating property

1. Introduction

With the rapid development of infrared detection equipment and infrared-guided weapons, infrared low-emissivity coatings (IRLECs) have become a hot topic [1]. The coatings are comprised of three components: additives, fillers, and adhesives [2]. Metal filler has the best performance, strong reflectivity to visible light, and good infrared stealth performance, but it is not beneficial to visible stealth. Aluminum is the most widely used because of its low cost, easy access, and good performance. Shi et al. investigated the influences of the floating rate of Al particles on the infrared emissivity [3].

The realization of infrared stealth performance mainly focuses on the properties of fillers. Liu et al. investigated high-emissivity composite-oxide fillers for a high-temperature-stable aluminum-chromium phosphate coating and analyzed the effects of the sintered fillers on emissivity [4]. Yan et al. investigated the effects of the aluminum mass fraction on the performance of an epoxy-lacquer-based coating [5]. Sometimes, additives are required in order to improve the infrared performance. Wang et al. investigated modification of Al pigment with graphene for infrared/visual stealth compatible fabric coating [6]. Low emissivity is the key index of IRLECs [7]. Gloss control in IRLECs with good mechanical and corrosion resistance has always been a research hotspot [8]. The high conformability of the carbon black paste has led to its wide use as an additive [9]. Fluorine-doped coatings appear to have excellent potential to obtain both corrosion protection and surface stability without adversely affecting mechanical properties [10]. The purpose of this paper was to modify the fluorine resin/aluminum infrared coating by quantitatively changing the amount of black paste, and to explore the effects of this kind of modification on gloss,

color difference, infrared emissivity, hardness, adhesion, impact resistance, roughness, optical testing, and corrosion resistance, then to obtain the black paste content when infrared emissivity is low.

2. Experimental

2.1. Experimental Materials

Fluorine resin (JF100) and curing agent: Juhua Group Co., Ltd., Quzhou, China. 4017 Al powder: Zhangqiu Metal Pigment Co., Ltd., Zhangqiu, China. Aluminum plate: 100 mm × 50 mm × 1 mm, Nanjing Chengxiang Aluminum Co., Ltd., Nanjing, China.

Other auxiliary materials: black paste (nano-slurry black 9927) was provided by Shenzhen Zhiyigao Co., Ltd., Shenzhen, China. Carbon black pigments were added to solvents such as propylene glycol methyl ether acetate, compound dicarboxylic acid, and butyl acetate, and then ground with a special structure hyperdispersant, rheological agent, and thixotropic agent. Carbon black pigment content was 20%, and particle size was nanometer grade (100 ± 15 nm).

2.2. Preparation of Coating

Abrasive papers (400 mesh) were used to grind the substrates, and alcohol was used to clean the substrates. Then, the pretreated substrates were dried in an oven. Before depositing, a high-pressure spray gun was used to clean the dust on the surface of the substrate. Nano-slurry black 9927 was added to coatings with a fixed ratio of Al powder and fluorine resin in accordance with the predetermined amount. After mixing, the coating was deposited on the surface of the pretreated aluminum plate (100 mm × 50 mm × 1 mm) using an SZQ tetrahedral fabricator (Tianjin Jinghai Science and Technology Testing Machinery Factory, Tianjin, China). The pretreated aluminum plate was fixed on the platform. Then, the prepared coatings were poured in front of the fabricator. The two ends of the fabricator were grasped by hand, then glided at a uniform speed of 150 mm/s, and the required thickness of the coating could be deposited. After 30 min for natural drying, the coating was ground using 1000-mesh abrasive papers, then a dry cloth was used to wipe off the dust. The coating preparation process needed to be repeated twice. Coatings were solidified at 40 °C for 2 h in a blast dryer (Taizhou Hengyou Electric Heating Equipment Manufacturing Co., Ltd., Taizhou, China). The thickness of the coatings was about 60 μm.

In the preliminary experiment, the ratio of the quantity of fluorine resin to the quantity of curing agent was 10:1. The quantity of aluminum powder/(aluminum powder + fluorine resin + curing agent) was 40% (weight percentage). (Fluorine resin + curing agent)/(aluminum powder + fluorine resin + curing agent) was 60%. The quantity of black paste/(aluminum powder + fluorine resin + curing agent + black paste) was 0%, 1.0%, 3.0%, 5.0%, 7.0%, 9.0%, and 10.0%. Variables are shown in Table 1.

Table 1. Composition of different pigments.

No.	Content of Nano-Slurry Black (%)	Quantity of Aluminum Powder (g)	Quantity of Fluorine Resin + Curing Agent (g)	Quantity of Black Paste (g)
1	0	2.00	3.00	0
2	1.0	1.98	2.97	0.05
3	3.0	1.94	2.91	0.15
4	5.0	1.90	2.85	0.25
5	7.0	1.86	2.79	0.35
6	9.0	1.82	2.73	0.45
7	10.0	1.80	2.70	0.50

2.3. Test and Characterization

The surface structure and morphology of the coatings were characterized by a JSM-5610LV scanning electron microscope, FEI Company, Hillsboro, OR, USA. The hardness of the coatings was tested by

QHQ-A coating hardness meter, Dongguan Huaguo Precision Instrument Co., Ltd., Dongguan, China. The hardness of the coatings was measured by a coating hardness tester with 6H–6B pencils. In the hardness test, the angle between the pencil and the coating was 45°, and the pencil scratched under a 1.0 kg load. The hardness of the coatings (determined with 6H, 5H, 4H, 3H, 2H, 1H, HB, 1B, 2B, 3B, 4B, 5B, and 6B pencils) was measured when scratches appeared on the coatings. The hardness of the pencil represents the hardness of the coating. The infrared emissivity of the coating in the range of 8–14 μm was tested by a Bruker Vertex 70 infrared emissivity tester, Chinese Academy of Sciences Shanghai Institute of Technological Physics, Shanghai, China. The chromatic values of the coatings were measured by a HP-2136 colorimeter, Zhuhai Tianchuang Instrument Co., Ltd., Zhuhai, China. L^* , a^* , and b^* are expressed as lightness, change of red and green color, and change of yellow and blue color, respectively. L_1^* , a_1^* , and b_1^* are the chromatic values of the substrate, while L_2^* , a_2^* , and b_2^* are the chromatic values of the deposited substrate. ΔL^* (brightness difference) = $L_1^* - L_2^*$, Δa^* (red and green difference) = $a_1^* - a_2^*$, and Δb^* (yellow blue difference) = $b_1^* - b_2^*$. The color difference is calculated by the following Formula (1):

$$\Delta E^* = [(\Delta L^*)^2 + (\Delta a^*)^2 + (\Delta b^*)^2]^{1/2}. \quad (1)$$

The gloss of the coating was tested by a BGD512-60° vancometer, Shenzhen Sanenshi Technology Co., Ltd., Shenzhen, China. The roughness of the coating was measured by a JB-4C precision roughness tester, Shanghai Taiming Optical Instrument Co., Ltd., Shanghai, China. The impact resistance of the coating was tested by a QCG paint film impact tester, Tianjin Precision Material Experiment Machine Factory, Tianjin, China. The heavy hammer was 1000 ± 1 g, the drawing scale was 50 cm in total and 1 cm in degree. The impact resistance of the coating is indicated by the maximum height of the hammer which is subjected to elongation deformation of the coating and does not cause damage when a hammer weight of a certain quality falls on the film. The corrosion resistance of the coating was tested by a CHI660E electrochemical workstation (Beijing Huakoputian Technology Co., Ltd., Beijing, China) and salt water immersion test. Electrochemical tests were carried out using a three-electrode battery structure. A saturated calomel electrode was used as the reference electrode and a platinum electrode as the counter electrode. The samples were immersed in 3.5% NaCl solution. After the open-circuit potential was stabilized, Tafel polarization tests were carried out. The test range was open-circuit potential ±0.3 V. The color of the coating was tested by a SEGT-J colorimeter, Guangzhou Biaogeda Experimental Instruments Co., Ltd., Guangzhou, China. The adhesion of the coating was tested by a QFH coating adhesion meter, Dongguan Huaguo Precision Instrument Co., Ltd., Dongguan, China. The samples were placed on a platform. The multi-edged cutting knife was placed perpendicular to the specimen plane using a hand-held gripper handle. The cutting speed was 20–50 mm/s with uniform pressure. Then, the coating was rotated 90° and the above operation on the cut to form a lattice pattern was repeated. The tape was attached to the entire grid and then was torn off at a minimum angle. A magnifying glass was used to observe the damage of the coating. The adhesion grade of the coating was determined according to the damage degree. There were six grades (0, 1, 2, 3, 4, and 5) in total. Grade 0 was the best adhesion, and grade 5 was the worst adhesion.

3. Results and Discussion

From Figure 1, it can be found that the surface gloss of fluorine resin coatings was below 25% after adding black paste, reaching sub-gloss. At the same time, as the content of black paste increased, the gloss of the coating surface decreased, and the decline rate kept constant. The main component of black paste was carbon black [11], which had large particle size and uneven particle size [12]. The higher the content of black paste, the higher the degree of uneven particle size, and the number of particles in the coating increased, so the gloss was lower [13].

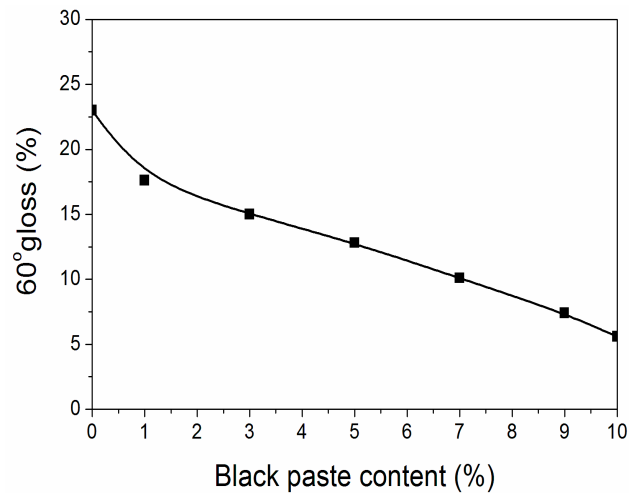


Figure 1. Effect of black paste content on gloss of the coatings.

As shown in Table 2 and Figure 2, the L_2^* value of the coatings decreased as the amount of black paste increased. At the same time, when the content of black paste increased from 0% to 9.0%, the ΔE^* value of the coating decreased to 6.7. When the content of black paste increased from 9.0% to 10.0%, the color difference increased slightly from 6.7 to 9.6. The color development of pigments was the result of the action of light on their chromogenic and assistant groups [14]. The size of pigment particles also had a great influence on its color performance, in order to ensure that a small amount of color matching reaction was consistent. In a certain range, both the particle size of the pigments and the covering power increased [15]. The smaller the particle size, the larger the specific surface area; the more lights energy absorbed; the smaller the fineness; the higher the dyeing power. Flocculation occurs easily when there are too many small particles [16].

Table 2. Color analysis results with different formulations.

No.	L_1^*	a_1^*	b_1^*	L_2^*	a_2^*	b_2^*	ΔE^*
1	25.9	5.2	-3.1	67.8	1.1	-2.3	42.1
2	25.9	5.2	-3.1	54.6	2.8	3.3	29.5
3	25.9	5.2	-3.1	43.9	2.5	5.5	20.1
4	25.9	5.2	-3.1	31.9	2.5	5.0	10.4
5	25.9	5.2	-3.1	28.0	2.3	5.7	9.5
6	25.9	5.2	-3.1	23.5	3.0	2.7	6.7
7	25.9	5.2	-3.1	21.8	2.3	5.1	9.6

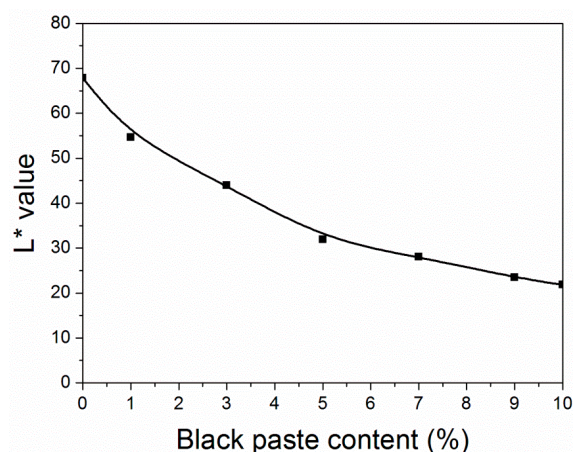


Figure 2. Effect of black paste content on the L^* value of the coatings.

From Figure 3, it can be seen that the infrared emissivity of fluorine resin coatings increased linearly with the increase of black paste content. It can be seen that the content of black paste had a significant effect on the infrared emissivity of the coating surface, which increased the infrared emissivity of the fluorine resin coating surface. After the infrared light was applied to the coating, it passed through the film-forming material containing the black paste, which absorbed the infrared light and thus increased the emissivity. The transmission of infrared light reached the surface of the aluminum powder, which was reflected by the aluminum powder and absorbed by the black paste. The color of the coating increased the infrared emissivity [17]. When the content of black paste was less than 3.0%, the coating had lower infrared emissivity.

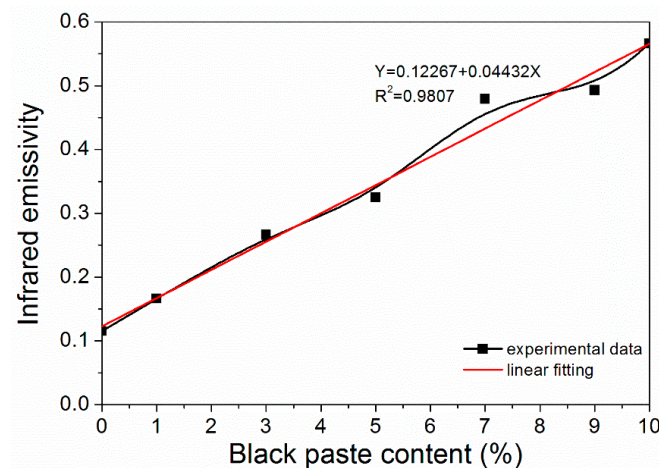


Figure 3. Effect of black paste content on the infrared emissivity of the coatings.

According to the experiment, when the content of black paste was from 0% to 10.0%, the hardness of all fluorine resin coatings was 6H. The hardness of the coating was not affected by the addition of black paste on the surface, and the coating could be completely cured. As shown in Figures 4 and 5, when the content of black paste was 0%–9.0%, the adhesion grade of the coating was grade 0; when the content was 10.0%, the adhesion grade was grade 1. The low density of aluminum powder and the high floating force in the coating made the aluminum powder distribute more on the surface of the coating [18]. As a result, the carbon black particles in the color paste distributed relatively less on the surface of the coating and were not uniform. Therefore, the black paste increased to 10.0%, which decreased the adhesion of the coating to the substrate [19].

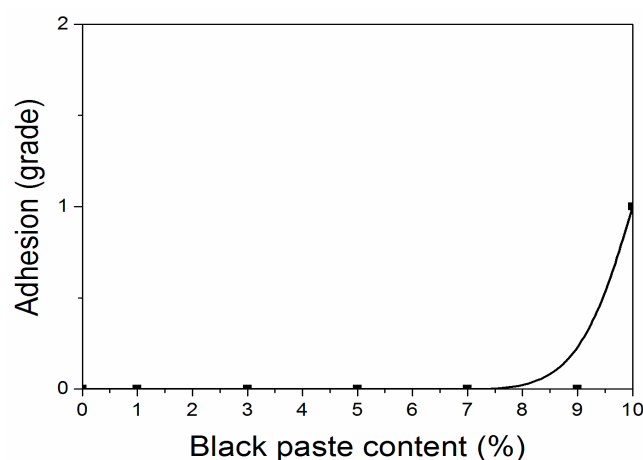


Figure 4. Influence of black paste content on adhesion of the coatings.

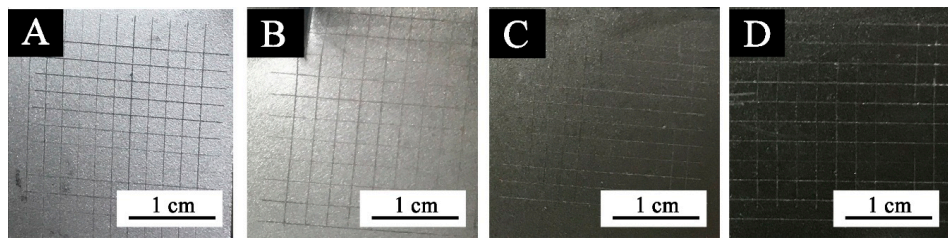


Figure 5. Images of coatings with different black paste content after adhesion test: (A) 0, (B) 1.0%, (C) 7.0%, and (D) 10.0%.

Figures 6 and 7 show that when the black paste content was between 0% and 3.0%, the impact resistance was 50 kg·cm, and the impact resistance was high. When the content of black paste was 10.0%, the impact resistance was the smallest. The addition of black paste was higher than 5.0%, and the impact resistance of the coating was worse with the increase of black paste content. This was because as more carbon black was added to the surface, the solid content of the coating increased and the relative resin content decreased. The powder state of the coating was enhanced, resulting in the decrease of impact resistance [20].

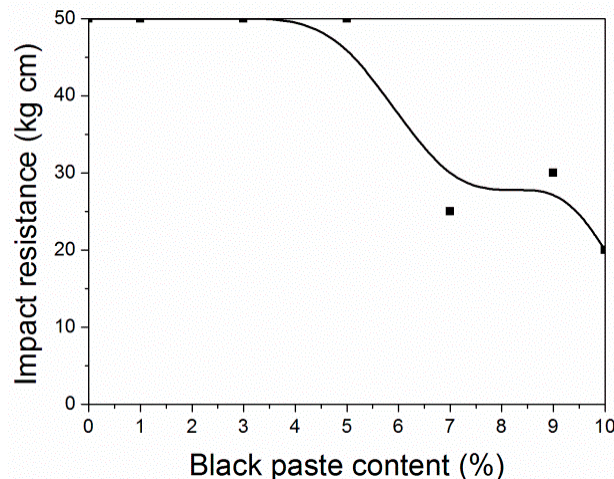


Figure 6. Effect of black paste content on the impact resistance of the coatings.

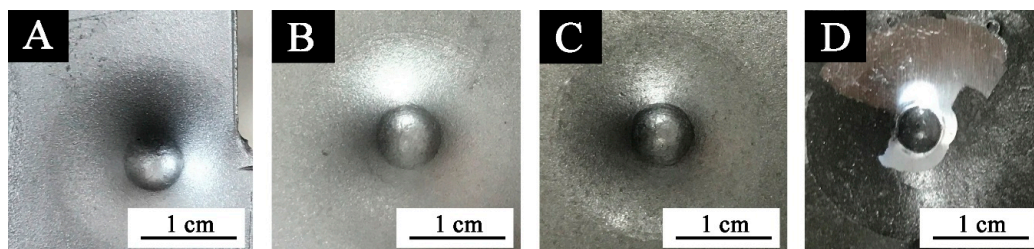


Figure 7. Images of coatings with different black paste content after impact resistance test: (A) 0%, (B) 1.0%, (C) 7.0%, and (D) 10.0%.

From Figure 8, it can be seen that when the content of black paste was 0%–5.0%, the surface roughness (R_a) of the coatings was relatively low, and the coatings were smooth. When the content of black paste was 5.0%–10.0%, the surface roughness of the coating was higher, and the roughness of the coating increased with the increase of the content of black paste. This was due to the uneven distribution of a large number of carbon black particles and the uneven surface of the coating, resulting in an increase in roughness [21].

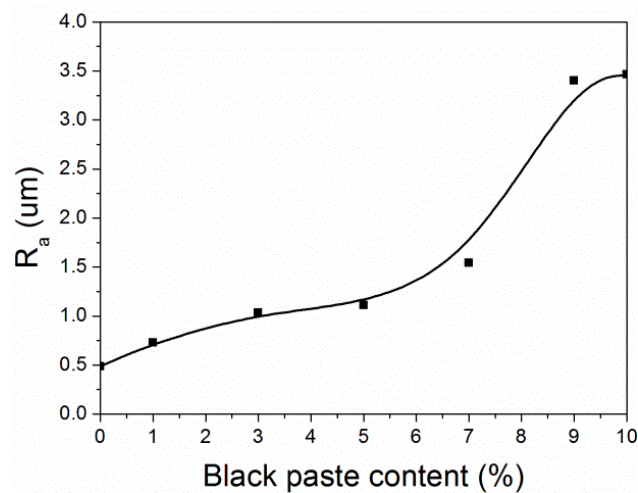


Figure 8. Effect of black paste content on the roughness of the coatings.

It can be seen from Figure 9 that when the content of black paste increased from 1.0% to 7.0% and 10.0%, the infrared absorption peak increased gradually, which was beneficial to reducing the surface reflectivity, thus increasing the absorption in the near-infrared band, resulting in an increase in infrared emissivity [22].

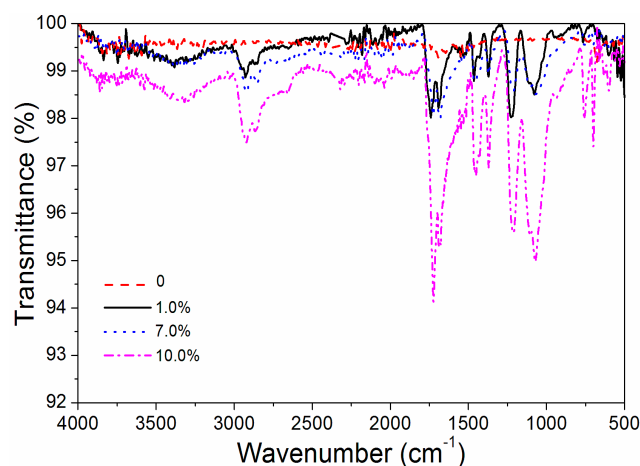


Figure 9. Influence of black paste content on the infrared spectra of the coatings.

The mechanical properties, optical properties, and infrared spectroscopy tests showed that the black paste yielded better properties when its content was 0%–3.0%. Therefore, the corrosion resistance of the coatings corresponding to 0%, 1.0%, and 3.0% black paste was tested. Aluminum sheets with three black paste contents were tested in brine, and the data of Figure 10 and Table 3 were obtained.

The higher the potential E_{corr} (V), the larger the resistance R_p (Ω/cm^2); and the smaller the current I_{corr} (A/cm^2), the better the corrosion resistance. The performance of the fluorine resin coating was the best when the content of black paste was 1.0% (Table 3). It can also be seen from the scanning electron microscopy (SEM) in Figure 11 that the addition of black paste affected the compactness of the coating [23]. Carbon black in black paste was added to coatings as an inorganic powder filler. When it was combined with fluorine resin to form coatings, due to the influence of surface shape, particle size, surface wetting agent, and solvent in the coating system, there were many pores between resin and carbon black, which affected the compactness of the whole coating. The more carbon black that was added, the more serious the defect between the resin and carbon black was, which affected the resistance of the coating to moisture and oxygen permeation [24].

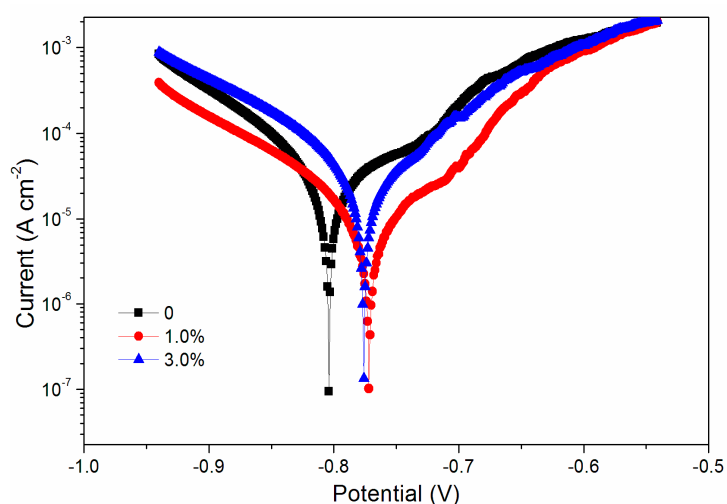


Figure 10. Tafel curve of coatings with different black paste contents.

Table 3. Effect of black paste content on corrosion resistance.

Content.	E_{corr} (V)	R_p (Ω/cm^2)	I_{corr} (A/cm^2)	β_a (mV/dec)	β_c (mV/dec)
0%	−0.804	670.2	2.791×10^{-5}	72.75	105
1.0%	−0.772	1899.8	8.821×10^{-6}	56.3	122
3.0%	−0.776	639.7	3.582×10^{-5}	90.34	127

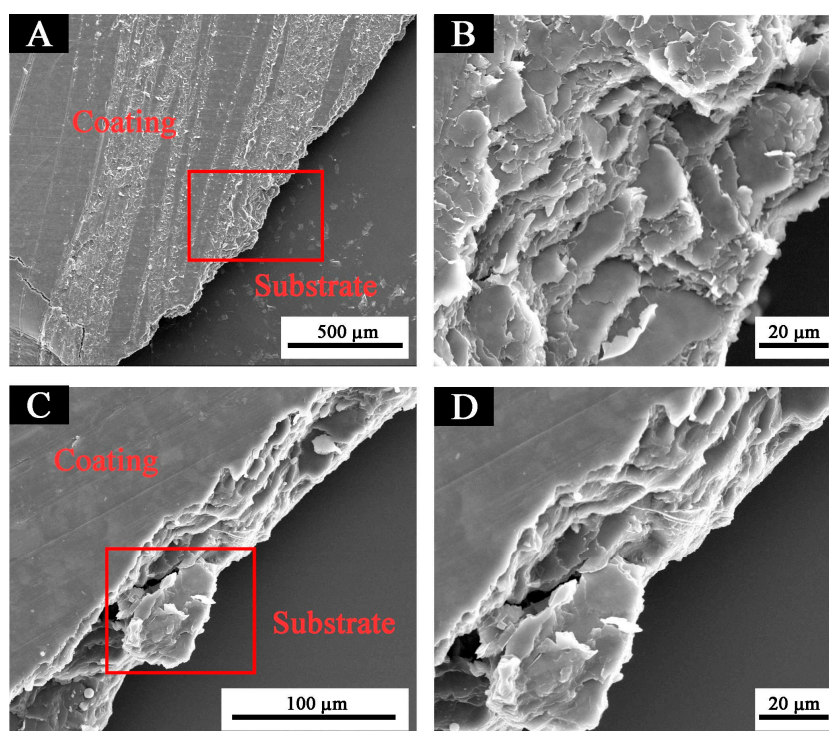


Figure 11. Cross-section scanning electron microscopy of coatings with different black paste contents coating: (A) 1.0% and (C) 3.0%. (B) and (D) are the zoomed views of the red boxes in (A) and (C), respectively.

4. Conclusions

By changing the content of black paste and keeping a fixed ratio of aluminum powder and fluorine resin, coatings with low infrared emissivity, low sub-gloss, low brightness, good adhesion, impact

resistance, and low roughness were prepared. When the content of black paste was 1.0%, the gloss and lightness of the whole fluorine resin coating was low; when the content of black paste was 1.0%, the fluorine resin coating had better adhesion, lower roughness, and better impact resistance. Considering all kinds of properties, when the content of black paste was 1.0%, fluorine resin coatings with good comprehensive properties, such as low infrared emissivity and low gloss, could be obtained.

Funding: This research received no external funding.

Acknowledgments: This project is supported by the Natural Science Foundation of Jiangsu Province (BK20150887), and Youth Science and Technology Innovation Fund of Nanjing Forestry University (CX2016018).

Conflicts of Interest: The author declares that there is no conflict of interest regarding the publication of this paper.

References

1. He, L.H.; Zhao, Y.; Xing, L.Y.; Liu, P.G.; Zhang, Y.W.; Wang, Z.Y. Low infrared emissivity coating based on graphene surface-modified flaky aluminum. *Materials* **2018**, *11*, 1502. [[CrossRef](#)] [[PubMed](#)]
2. Liang, J.; Li, W.; Xu, G.Y.; Meng, X.; Liu, K.; Tan, S.J. Preparation and characterization of the colored coating with low infrared emissivity based on nanometer pigment. *Prog. Org. Coat.* **2018**, *115*, 74–78. [[CrossRef](#)]
3. Shi, M.Y.; Xu, C.; Yang, Z.H.; Liang, J.; Wang, L.; Tan, S.J.; Xu, G.Y. Achieving good infrared-radar compatible stealth property on metamaterial-based absorber by controlling the floating rate of Al type infrared coating. *J. Alloy. Compd.* **2018**, *764*, 314–322. [[CrossRef](#)]
4. Liu, Z.K.; Sun, Q.; Song, Y.; Yang, J.; Chen, X.Q.; Wang, H.R.; Jiang, Z.H. High-emissivity composite-oxide fillers for high temperature stable aluminum-chromium phosphate coating. *Surf. Coat. Technol.* **2018**, *349*, 885–893. [[CrossRef](#)]
5. Yan, X.X.; Cai, Y.T.; Lu, R.; Miyakoshi, T. Development and characterization of new coating material of blended epoxy-lacquer with aluminum. *Int. J. Polym. Sci.* **2017**, *2017*, 5017356. [[CrossRef](#)]
6. Wang, K.Z.; Wang, C.X.; Yin, Y.J.; Chen, K.L. Modification of Al pigment with graphene for infrared/visual stealth compatible fabric coating. *J. Alloy. Compd.* **2017**, *690*, 741–748. [[CrossRef](#)]
7. Liu, J.; Ji, H.H. Experimental investigation on infrared signatures of axisymmetric vectoring exhaust nozzle with film cooling and low-emissivity coating. *J. Eng. Gas Turb. Power* **2018**, *140*, 091203. [[CrossRef](#)]
8. Qiao, Z.; Mao, J. Multifunctional poly (melamine-urea-formaldehyde)/graphene microcapsules with low infrared emissivity and high thermal conductivity. *Mater. Sci. Eng. B Adv.* **2017**, *226*, 86–93. [[CrossRef](#)]
9. Hu, K.S.; Chung, D.D.L. Flexible graphite modified by carbon black paste for use as a thermal interface material. *Carbon* **2011**, *49*, 1075–1086. [[CrossRef](#)]
10. Bakhsheshi-Rad, H.R.; Hamzah, E.; Kasiri-Asgarani, M.; Jabbarzare, S.; Iqbal, N.; Kadir, M.R.A. Deposition of nanostructured fluorine-doped hydroxyapatite-polycaprolactone duplex coating to enhance the mechanical properties and corrosion resistance of Mg alloy for biomedical applications. *Mat. Sci. Eng. C Mater.* **2016**, *60*, 526–537. [[CrossRef](#)]
11. Ibanez-Redina, G.; Silva, T.A.; Vicentini, F.C.; Fatibello, O. Effect of carbon black functionalization on the analytical performance of a tyrosinase biosensor based on glassy carbon electrode modified with dihexadecylphosphate film. *Enzyme Microb. Technol.* **2018**, *116*, 41–47. [[CrossRef](#)] [[PubMed](#)]
12. Gueli, A.M.; Bonfiglio, G.; Pasquale, S.; Troja, S.O. Effect of particle size on pigments colour. *Color Res. Appl.* **2017**, *42*, 236–243. [[CrossRef](#)]
13. Valdesueiro, D.; Hettinga, H.; Drijfhout, J.P.; Lips, P.; Meesters, G.M.H.; Kreutzer, M.T.; van Ommen, J.R. Tuning roughness and gloss of powder coating paint by encapsulating the coating particles with thin Al₂O₃ films. *Powder Technol.* **2017**, *318*, 401–410. [[CrossRef](#)]
14. da Silva, R.M.; Tebcherani, S.M.; Kubaski, E.T.; Cava, S.; Moreira, M.L.; Sequinel, T. Development of a yellow pigment based on bismuth and molybdenum-doped TiO₂ for coloring polymers. *Int. J. Appl. Ceram. Technol.* **2015**, *12*, E112–E119. [[CrossRef](#)]
15. Kong, S.H.; Shore, J.D. Modeling the impact of silver particle size and morphology on the covering power and tone of photothermographic media. *J. Imaging Sci. Technol.* **2007**, *51*, 235–242. [[CrossRef](#)]
16. Pan, W.L.; Zhou, Y.M.; He, M.; Bu, X.H.; Ding, B.B.; Huang, T.Y.; Huang, S.; Li, S.W. Synthesis, helicity, and low infrared emissivity of optically active poly(N-propargylamides) bearing stigmasteryl moieties. *J. Mol. Struct.* **2017**, *1142*, 285–292. [[CrossRef](#)]

17. Liu, Y.F.; Xie, J.L.; Luo, M.; Peng, B.; Xu, C.; Deng, L.J. The synthesis and optical properties of Al/MnO₂ composite pigments by ball-milling for low infrared emissivity and low lightness. *Prog. Org. Coat.* **2017**, *108*, 30–35. [[CrossRef](#)]
18. Olakanmi, E.O. Effect of mixing time on the bed density, and microstructure of selective laser sintered (SLS) aluminium powders. *Mater. Res. Ibero Am. J.* **2012**, *15*, 167–176. [[CrossRef](#)]
19. Kozlova, A.A.; Kondrashov, E.K.; Deev, I.S. Protective properties of paint and lacquer coatings based on a fluorine-containing film-forming material. *Prot. Met. Phys. Chem.* **2016**, *52*, 1181–1186. [[CrossRef](#)]
20. Olah, A.; Croitoru, C.; Tierean, M.H. Surface properties tuning of welding electrode-deposited hardfacings by laser heat treatment. *Appl. Surf. Sci.* **2018**, *438*, 41–50. [[CrossRef](#)]
21. Salca, E.A.; Krystofiak, T.; Lis, B. Evaluation of selected properties of alder wood as functions of sanding and coating. *Coatings.* **2017**, *7*, 176. [[CrossRef](#)]
22. Sanamzadeh, M.; Tsang, L.; Johnson, J.T.; Burkholder, R.J.; Tan, S.R. Scattering of electromagnetic waves from 3D multilayer random rough surfaces based on the second-order small perturbation method: energy conservation, reflectivity, and emissivity. *J. Opt. Soc. Am. A* **2017**, *34*, 395–409. [[CrossRef](#)] [[PubMed](#)]
23. Wu, C.Y.; Zhang, J. Corrosion protection of Mg alloys by cathodic electrodeposition coating pretreated with silane. *J. Coat. Technol. Res.* **2010**, *7*, 727–735. [[CrossRef](#)]
24. Wang, L.H. Compressive capacitance relaxation of carbon black filled silicone rubber composite. *Polym. Compos.* **2018**, *39*, 3446–3451. [[CrossRef](#)]



© 2019 by the author. Licensee MDPI, Basel, Switzerland. This article is an open access article distributed under the terms and conditions of the Creative Commons Attribution (CC BY) license (<http://creativecommons.org/licenses/by/4.0/>).